

Kinetic Study of the Formation of Dihydrogen from the Reaction of [1.1]Ferrocenophanes with Strong Acids

Manny Hillman,* Sherie Michaille, and Stephen W. Feldberg*

Chemical Sciences Division, Department of Applied Science, Brookhaven National Laboratory,
Upton, New York 11973

John J. Eisch

Department of Chemistry, State University of New York at Binghamton, Binghamton, New York 13901

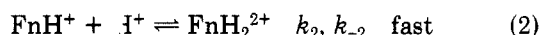
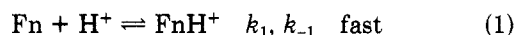
Received October 5, 1984

The kinetics of the reactions of [1.1]ferrocenophane, I, 3,3'-trimethylene[1.1]ferrocenophane, II, and 2,2'-trimethylene[1.1]ferrocenophane, III, with very strong acids were studied by using electrochemical techniques. Catalytic currents were obtained from the reduction of the dications of the ferrocenophanes at a mercury electrode in various concentrations of BF_3 in H_2O . The overall rate constants for the formation of dihydrogen from I and II are first order in the ferrocenophane concentration. The inverses of the overall rate constants exhibit quadratic dependences on the inverse acid strengths. These measurements, together with the information obtained from cyclic voltammograms, are consistent with a three-step mechanism for the formation of dihydrogen: two protonation steps followed by the elimination of dihydrogen as the rate-determining step at the highest acid strengths used. The rate of dihydrogen formation from III was too slow to measure with this electrochemical technique. The relative values of the rate constants for dihydrogen elimination are correlated with the structures of the ferrocenophanes, their flexibility, and the probable orientation of the protons on the iron atoms. The rates are in the order of $\text{II} > \text{I} \gg \text{III}$.

Introduction

Bitterwolf and Ling¹ reported that compound I (see Figure 1 for the structures) reacts quantitatively with a strong acid, e.g., $\text{BF}_3 \cdot \text{H}_2\text{O}$, to yield the ferrocenophane dication and dihydrogen.¹ This reaction has been utilized to produce hydrogen gas catalytically at a modified p-type silicon electrode.²

In view of the importance of reactions that generate dihydrogen catalytically, we decided to investigate the mechanism of the reaction. Since ferrocene derivatives are known to be protonated on the iron atom under these conditions,^{3,4} it was assumed by the discoverers¹ that the mechanism involves stepwise protonation of the two iron atoms followed by elimination of dihydrogen with concurrent formation of the ferrocenophane dication (eq 1-3),



where Fn is the ferrocenophane. Theoretical calculations⁵ support this idea but suggest that the protonation of the iron may be preceded by protonation of a ring carbon.

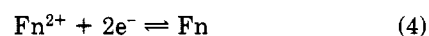
There are, however, other conceivable mechanisms. One, for example, might involve the reaction of a hydrogen atom of a [1.1] methylene group with the acid. Elimination of a hydride from that position has been demonstrated.⁶ A kinetic study might be able to demonstrate consistency

with one or more of the conceivable mechanisms. Other methods, e.g., tracer studies using deuterium, may be necessary to resolve some of the differences.

Several approaches to the study of the kinetics were explored by us: (a) tensiometry for the determination of the rate of dihydrogen evolution, (b) UV-visible spectrometry for the determination of the rate of formation of the ferrocenophane dication, (c) double-step chronoamperometry for the determination of the rate of the first protonation reaction, (d) chronoamperometry to measure the overall rate constant of the reaction, and (e) cyclic voltammetry for qualitative assessment of the potentials to be used in the chronoamperometry experiments and for other ancillary purposes. The last two techniques are more fully described in the main parts of this paper.

Tensiometry proved to be virtually impossible at the high acid strengths because the acid itself has a significantly high vapor pressure and the differences between the background pressures and the increases in pressure due to dihydrogen evolution are very small. Spectrometry, attempted by placing the solid ferrocenophane into the neat acid, proved impractical because dissolution of the ferrocenophane in the acid is slow compared to the rate of the reaction. The use of a mutual solvent proved difficult since the best solvent found, 2,4-dimethylsulfolane, and the acids are both quite viscous, and a significant time is consumed in mixing the components. The problems of using tensiometry and spectrometry appear now to be solvable, but for much lower acid strengths than those used in the present report.

Because of the difficulties with these techniques at high acidities, we turned our attention to the electrochemical methods in which the reduction of Fn^{2+} to Fn occurs at a mercury electrode (eq 4), and the reactions of eq 1-3 take place in the solution near the electrode regenerating Fn^{2+} to complete the cycle.



We also examined the effects of structural modifications in the ferrocenophane on the reaction rates.

(1) Bitterwolf, T. E.; Ling, A. C. *J. Organomet. Chem.* 1973, 57, C17-C18.

(2) Mueller-Westerhoff, U. T.; Nazzal, A. I. *J. Am. Chem. Soc.* 1984, 106, 5381-5382.

(3) Curphy, T. J.; Santer, J. O.; Rosenblum, M.; Richards, J. H. *J. Am. Chem. Soc.* 1960, 82, 5249-5250.

(4) Bitterwolf, T. E.; Ling, A. C. *J. Organomet. Chem.* 1972, 40, 197-203.

(5) Waleh, A.; Loew, G. H.; Mueller-Westerhoff, U. T. *Inorg. Chem.* 1984, 23, 2859-2863.

(6) Mueller-Westerhoff, U. T.; Nazzal, A.; Prossdorf, W.; Mayerle, J. J.; Collins, R. L. *Angew. Chem., Int. Ed. Engl.* 1982, 4, 293-294.

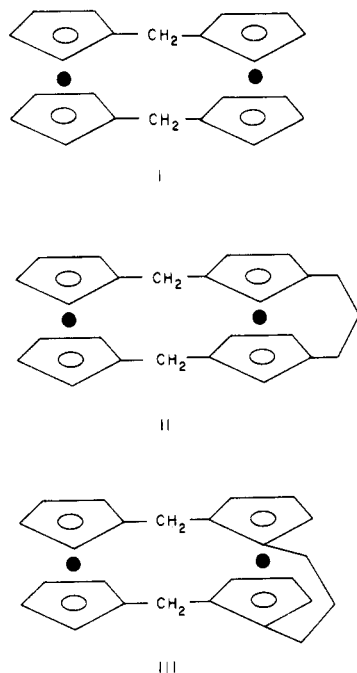


Figure 1. Structural representations of compounds used in this study. The filled circles are the iron atoms.

Electrochemical Analysis

A schematic representation of a catalytic reaction scheme (see Bard⁷) is shown in eq 5 and 6. In our case,



the multistep mechanism can be reduced to eq 5 and 6 by setting $[A] = [Fn^{2+}]$, $[B] = [Fn] + [FnH^+] + [FnH_2^{2+}]$, and, for the steady-state condition, k_m is the overall first-order or pseudo-first-order rate constant. k_m can be derived in terms of $K_1 = k_1/k_{-1}$, $K_2 = k_2/k_{-2}$, k_1 , k_2 , and k_3 as

$$\frac{1}{k_m} = \frac{1}{k_3} + \left(\frac{1}{k_3 K_2} + \frac{1}{k_2} + \frac{1}{k_1} \right) \frac{1}{[H^+]} + \left(\frac{1}{K_1 K_2 k_3} + \frac{1}{K_1 k_2} \right) \frac{1}{[H^+]^2} \quad (7)$$

The dehydrogenation rate constant, k_3 , can be determined unambiguously from a least-squares fit of the data of the overall rate constant, k_m , and acid strength, $-\log [H^+] = H_0$, to 7. The determination of the other rate constants and of the equilibrium constants is not as straightforward.

The details of the cyclic voltammetric and chronoamperometric techniques and the general behavior of the "catalytic" mechanism (eq 5 and 6) are reviewed elsewhere.⁷ The chemistry and the geometry of our system indicated that spherical diffusion could not be neglected in the analysis of the steady-state currents.

All our quantitative data were obtained by using chronoamperometry. With this technique, the catalytic mechanism will exhibit a time-dependent current that ultimately decays to a steady-state value. The equation for the steady-state flux must satisfy the differential equations describing the diffusion and kinetics of reactions 5 and 6 at a spherical electrode:

$$d[A]/dt = D_A(\partial^2[A]/\partial r^2 + (2/r)\partial[A]/\partial r) + k_m[B] \quad (8)$$

$$d[B]/dt = D_B(\partial^2[B]/\partial r^2 + (2/r)\partial[B]/\partial r) - k_m[B] \quad (9)$$

and

$$I = nF D_A (d[A]/dr)_{r=r_0} \quad (10)$$

where D_A and D_B are the diffusion coefficients of species A and B, r is the distance from the center of a spherical electrode of radius r_0 , F is the Faraday constant, a is the surface area of the electrode, and n is the number of electrons. For $D_A = D_B = D$, a common and reasonable assumption for similar species, and $[A]_{r=r_0} = 0$ (a boundary condition for the chronoamperometric experiment), the steady-state current taking spherical diffusion into account is described by⁸

$$I_{ss} = n a F C_A ((k_m D)^{1/2} + D/r_0) \quad (11)$$

where C_A is the bulk concentration of A. At short times ($t < 0.05$ s in our system), when $k_m t < 0.02$ and $(Dt)^{1/2}/r_0 < 0.02$, contributions to the current from sphericity and from kinetics can be ignored, and the time-dependent current is described by the Cottrell equation:⁷

$$I_t = n a F C_A (D/(\pi t))^{1/2} \quad (12)$$

A convenient evaluation of k_m is derived from eq 11 and 12:

$$k_m^{1/2} = (\pi t)^{-1/2} I_{ss}/I_t - D^{1/2}/r_0 \quad (13)$$

where the term $D^{1/2}/r_0$ appears as a correction term to the formulation for the planar electrode. In our experiments, the spherical correction ranged from 5 to 24%.

Experimental Section

The acids employed in this study were mixtures of $BF_3 \cdot H_2O$ and $BF_3 \cdot 2H_2O$ of known concentration prepared by the reaction of BF_3 gas (Matheson) with water.⁹ The dihydrate ($BF_3 \cdot 2H_2O$, $H_0 = -6.8$) is a much weaker acid than the monohydrate ($BF_3 \cdot H_2O$, $H_0 = -11.3$).⁹ The acid strengths of the mixtures were measured¹⁰ spectrophotometrically with a Carey 219 using 2,4,6-trinitroaniline, anthraquinone, and 2-bromo-4,6-dinitroaniline as Hammett indicators (Aldrich Chem. Co.).

Compound I was donated by Dr. U. T. Mueller-Westerhoff and was prepared in our laboratory by Mueller-Westerhoff's procedures.¹¹ Compounds II and III were prepared in our laboratory.¹² Weighed quantities of the compounds were transferred to a volumetric flask, and acid of known acid strength was added. As happens in such strong acids, the ferrocenophane is quantitatively oxidized to the dication prior to the electrochemical measurements. The concentrations of solutions used were generally 10^{-3} M.

The reaction solutions were deaerated by passing through N_2 for 5 min. Since the color contributed by the ferrocenophanium dication prevented the use of the indicators to measure the acid strengths after the mixtures were deaerated, deaerations were also performed on sample acids (without ferrocenophane but of known acid strengths) to determine the effect of deaerations on the acid strengths. The corrected acid strengths (0.8% at the highest acidities and negligible at the lower acidities) were used.

The electrochemistry was performed in an enclosed cell equipped with a nitrogen inlet to ensure exclusion of oxygen during the measurements. The three-electrode system used for the cell consisted of a hanging-mercury-drop working electrode (HMDE), a mercury-pool counter electrode, and a saturated calomel electrode (SCE) as a reference electrode. A fresh drop of mercury

(8) Saveant, J. M.; Vianello, E. *Electrochim. Acta* 1965, 10, 905-920.

(9) Vinnik, M. I.; Manelis, G. B.; Chirkov, N. M. *Zh. Neorg. Khim.* 1957, 7, 1643-1648.

(10) Hammett, L. P.; Deyrup, A. J. *J. Am. Chem. Soc.* 1932, 54, 2721-2739.

(11) Cassens, A.; Eilbracht, P.; Nazzari, A.; Prossdorf, W.; Mueller-Westerhoff, U. T. *J. Am. Chem. Soc.* 1981, 103, 6367-6372.

(12) Singletary, N. J.; Hillman, M.; Dauplaise, H.; Kwick, A.; Kerber, R. C. *Organometallics* 1984, 3, 1427.

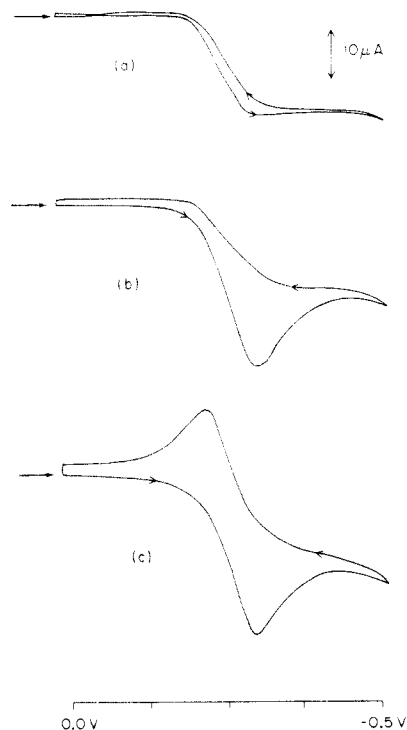


Figure 2. Cyclic voltammetry: (a) catalytic current at slow scan rate (5 mV s^{-1} ; $H_0 = -9.6$); (b) reduction wave, but no oxidation wave at faster scan rate (70 mV s^{-1} ; $H_0 = -9.6$); (c) reduction and oxidation waves at still faster scan rate at lower acid strength (100 mV s^{-1} ; $H_0 = -7.5$). The arrows indicate the starting points of the scans and the zero current lines.

was used for each experiment, and an interval of at least 30 s was allowed after the formation of each drop to ensure homogeneous and quiet conditions during measurement. The nature of our home-made hanging drop device precludes accurate control or reproducibility of the drop size. However, the drop size is constant during any given experiment.

The temperature was controlled to within $\pm 0.02 \text{ }^\circ\text{C}$ by a water-jacketed cell holder that was fed by a constant-temperature circulating bath. The kinetic studies of the variation of rate with acid strength were performed at $22.0 \text{ }^\circ\text{C}$.

Chronoamperometry⁷ and double-step chronoamperometry⁷ were carried out by using a Princeton Applied Research Model 173 potentiostat and Model 175 universal programmer. To measure current, the potential across a $1000 \text{ } \Omega$ resistor (installed with a stabilizing 45 nF capacitor) in series with the auxiliary electrode was fed directly into the differential input of a Nicolet Model 1090 digital oscilloscope. The data were stored on magnetic tape (Kennedy Model 9700) for later analysis. Cyclic voltammetry⁷ was performed with the above system or with an IBM EC/225 voltammetric analyzer, and voltammograms were plotted on a YEW Model 3022 XY recorder. The proper functioning of the cell and equipment was tested with an aqueous $1 \text{ mM Cd(NO}_3)_2$ solution with 1 M KNO_3 whose behavior at a HMDE is well documented.¹³

The potentials chosen for the chronoamperometry experiments were based on cyclic voltammetry results. The dications of I and II are reduced at approximately -220 mV . The acids begin to be significantly reduced at -550 mV . To verify that the reduction potential was sufficient to ensure diffusion control, the reduction potential was varied by increments of 50 mV over the range of -350 to -450 mV , and the results were shown to be independent of potential.

The pulse duration, τ , generally used was 20 s . The chronoamperogram was examined to ascertain that a steady state had been reached and to confirm that it was maintained for the duration of the pulse. The quantity $k_m \tau$, where k_m is the first-order rate constant for regeneration, was checked to ensure that it exceeded the value 1.5, the theoretical minimum value⁷ for the

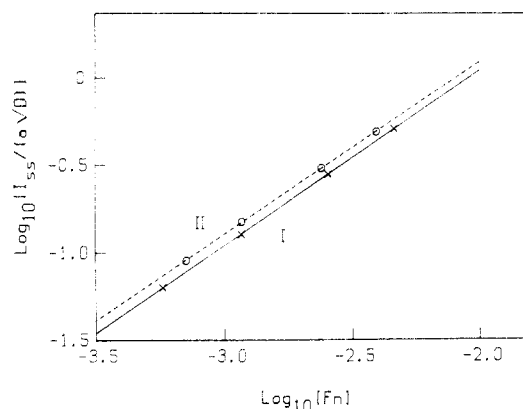


Figure 3. Reaction order determination. Slopes: I, 1.01 ± 0.09 ; II, 0.99 ± 0.09 .

attainment of a steady state. The term, $It^{1/2}$, virtually constant for $t < 0.05 \text{ s}$ since $k_m t < 0.02$ and the currents are diffusion controlled, was calculated from an average of values over the time interval from 10 to 50 ms.

Results

In acetonitrile, the cyclic voltammograms of [1.1]-ferrocenophanes exhibit two anodic and two cathodic peaks corresponding to two (nearly) reversible one-electron redox processes.^{12,14} In the strongly acidic conditions, $H_0 = -9.6$, used in this study, cyclic voltammetry at 70 mV s^{-1} exhibits a single reduction peak (Figure 2b) which corresponds (see below) to a two-electron process. Using slower scan rates (i.e., 5 mV s^{-1}) a steady-state current is observed (Figure 2a). This suggests a catalytic process where the dication is regenerated near the electrode by homogeneous chemical reactions (e.g., eq 1-3). The absence of an oxidation peak on the return cycle even at faster scan rates (Figure 2b) indicates that a very fast process is removing the reduced ferrocenophane from the reaction before it can be reoxidized at the electrode. Finally, at lower acidity, $H_0 = -7.5$, and at fast scan rates, 100 mV s^{-1} , the oxidation peak appears separated from the reduction peak by $60\text{--}70 \text{ mV}$ (Figure 2c).

We have presumed a pseudo-first-order catalytic regeneration of Fn^{2+} (eq 1-3). Thus, it is necessary to show that the reaction is first order with respect to ferrocenophane. Plots (Figure 3) of $\log(I_{ss}/aD^{1/2})$ vs. $\log(C_A)$ (eq 11) in the concentration range from 10^{-4} to 10^{-3} M exhibit slopes of 1.01 ± 0.09 for I and 0.99 ± 0.09 for II confirming first-order behavior.

It is also necessary to verify that the dication is reduced to the neutral ferrocenophane by a two electron process ($n = 2$). This can be determined by chronoamperometry from a plot of $I_t t^{1/2}$ vs. t (eq 12) using data from the time zone in which $I_t t^{1/2}$ is constant (i.e., $t < 0.05 \text{ s}$). Thus a value of $naD^{1/2}$ is obtained by using eq 12. To determine $aD^{1/2}$, a surrogate molecule can be used which is known to have a one-electron redox reaction and is believed to have a diffusion constant close to that of the ferrocenophane. It should be noted that, since the number of electrons is an integer, probably 1 or 2, the surrogate molecule need only have a diffusion coefficient within a factor of 2 of that of the ferrocenophane. Ferrocene is smaller than the ferrocenophane but was found to be an adequate surrogate. Benzylferrocene was even superior since it is similar in size to the ferrocenophane. An attempt was also made to use 1,1'-dibenzylferrocene which should

(13) Anson, F. C. *Anal. Chem.* **1966**, *38*, 54-57.

(14) Morrison, W. H.; Krogsrud, S.; Hendrickson, D. N. *Inorg. Chem.* **1973**, *12*, 1998-2004.

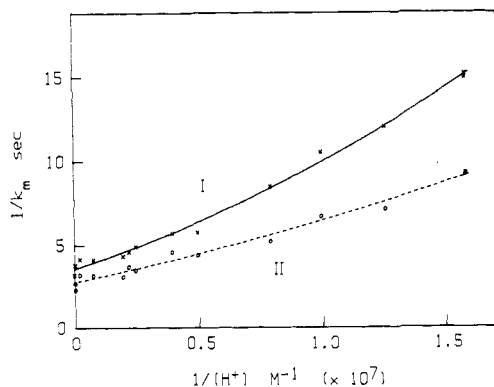


Figure 4. Acid dependence of overall rate constant, k_m .

Table I. Rate Constants, Equilibrium Constants (log), Activation Energies,^a and Frequency Factors^a (log)

	I	II
k_3, s^{-1}	0.28 (1)	0.36 (2)
pK_{a1}	-6.5 (1)	-6.3 (3)
pK_{a2}	-7.1 (1)	-7.0 (1)
$E_a, kcal\ mol^{-1}$	13.5 (5)	14.2 (7)
$\ln A, s^{-1}$	21.7 (7)	23.3 (11)

^a $H_0 = -9.5$; temperature range, 14–42 °C.

be larger than the ferrocenophane since the benzyl groups are probably on opposite sides of the ferrocene unit, but strong adsorption on the mercury electrode prevented a meaningful measurement. With these reasonable estimates for $aD^{1/2}$, the number of electrons involved in the electrode reduction of the ferrocenophane dications was determined as 2.0 ± 0.2 . Having established that the electrolytic reduction involves a two-electron change, the value of D was determined from chronoamperometric experiments ($H_0 = -8$ to -9 , ~ 1 mM in ferrocenophane) on a mercury pool electrode of known area. Corrections in D were made for small variations in the viscosities of the media using Stoke's law. Since C_A is accurately known, a good estimate of a and consequently of r_0 is obtained from eq 12.

The rate constant, k_m , for the overall regeneration of the oxidized species was then determined from eq 13. Plots (Figure 4) of $1/k_m$ vs. $1/[H^+]$ are given in Figure 4. A least-squares fit of $1/k_m$ vs. $1/[H^+]$ to a quadratic equation unambiguously yields the rate constant k_3 as the inverse of the constant term (eq 7). The determination of the other parameters in eq 7 from the other coefficients of the quadratic is not as straightforward and is described in the Discussion.

The overall rate constants, dehydrogenation rate constants, and equilibrium constants as determined for compounds I and II are given in Table I. The rate of reaction for compound III is too slow to be measured by this electrochemical technique.

The activation energies and the entropy changes of the reactions (Table I) were determined from the values of k_3 obtained at various temperatures (14–42 °C) for $H_0 = -9.5$. At this acid strength the overall rate constant, k_m , is virtually equal to the rate constant k_3 .

Discussion

Cyclic voltammetry confirmed that the catalytic reaction was taking place and confirmed that there was a fast reaction removing the reduced species from the electrochemical reaction since the oxidation wave could not be seen at high scan rates. Protonation of the iron atom of ferrocene is known to occur,^{3,4} and the cyclic voltammogram of the ferrocenium cation also does not exhibit an oxidation wave after reduction in this medium. We con-

clude, therefore, that protonation of the iron atoms of the ferrocenophane is the fast step that removes the ferrocenophane from possible oxidation at the electrode. Thus, this electrochemical behavior is in accord with the first step of the proposed mechanism.

Double-step chronoamperometry on a millisecond time scale was explored as a method for determining the rate of the first protonation, but adsorption of what was probably the reduced species on the electrode was a competing reaction, and the complications could not be overcome even by using dimethylsulfolane as a solvent. The fast process mentioned above that prevents reoxidation of the reduced species was not the adsorption. The oxidation wave of the adsorbed species would still appear, though with a different shape and position than expected. Despite the adsorption, chronoamperometry on a seconds time scale was useful for the slow reaction processes since the adsorption reaction could then be considered as one of any number of very fast reactions that do not enter the analysis.

Under neutral conditions, in nonoxidizing media, e.g., acetonitrile, the dication Fn^{2+} reacts with the reduced ferrocenophane, Fn , to give a monocation, Fn^+ . The possibility of this reaction taking place under the conditions of this study must be evaluated, for its existence would increase the curvature and slope in Figure 4 and, consequently, affect the determination of K_1 and K_2 . We can justify ignoring this reaction at the high acid strengths used in this study by noting that introduction of just Fn^+ into the acid resulted in extensive decomposition of the ferrocenophanium cation without formation of dihydrogen, while introduction of the neutral ferrocenophane into the acid gave a quantitative yield of dihydrogen. We would not be surprised if the conproportionation reaction became important at lower acid strengths. The effect of erroneously ignoring it, however, would be to give values of K_1 and K_2 that are too low, and, at the highest acid strengths, the dehydrogenation reaction would still be found to be the rate-determining step.

The values of the equilibrium constants of the protonation reactions can be obtained from the least-squares computations by introducing some approximations. If we assume that at these acid strengths the protonations are relatively fast, specifically that k_1 and k_2 are large compared to k_3K_2 , eq 7 can be simplified to give

$$\frac{1}{k_m} = \frac{1}{k_3} + \frac{1}{K_2 k_3 [H^+]} + \frac{1}{K_1 K_2 k_3 [H^+]^2} \quad (14)$$

The equilibrium constants K_1 and K_2 may then be determined in a straightforward way.

The values for the equilibrium constants obtained in this way, pK_{a1} and pK_{a2} (Table I), are in the neighborhood of the value of the pK_a of -6.6 reported¹⁵ for ferrocene. They are also in the relative sizes expected, with the equilibrium constant of the first protonation greater than the second. These results support the assumption that the protonation reactions are relatively fast, at least at these acid strengths. This conclusion might be somewhat surprising since the second protonation involves an interaction of two positively charged species. The relative ease of the two protonations can be correlated with the relative ease of removal of two electrons from the ferrocenophane under neutral conditions in acetonitrile.^{12,14} For I, the two potentials differ by 200 mV, indicating a small difference in ease of removal of the first and second electron. Moreover, the second

potential differs from the redox potential of ferrocene by ~ 100 mV, indicating that the ease of removal of the second electron is not much different from removal of an electron from ferrocene. That this occurs has been taken as a lack of significant interaction between the two ferrocene units. By contrast, in [0.0]ferrocenophane, where the interaction between the two units has been demonstrated for the monocation,¹⁶ the two redox potentials¹⁴ differ by 590 mV. Furthermore, under the high acid strengths used in these studies, the first and second redox potentials for the ferrocenophanes differ by much less, as indicated by the single wave observed in the cyclic voltammograms. Since protonation is analogous to an oxidation reaction, the ease of effecting the second protonation should be not much less than that of the protonation of ferrocene.

The equilibrium constants for the protonation reactions, the activation energies, and the entropy factors for the dehydrogenation reactions (Table I) were not determined with sufficient precision to differentiate between compounds I and II. Consequently no insight into the difference can be gained from these results. Improved equilibrium constants can probably be obtained at lower acid strengths by using the tensiometric and spectrometric techniques discussed above.

The two types of reactions in the proposed mechanism, protonation of an iron atom and formation of a dihydrogen molecule, involve two different structural considerations. The protonation reactions require that the pairs of cyclopentadienyl rings of each ferrocene unit become mutually tilted at some undetermined dihedral angle.^{17,18} The formation of the dihydrogen molecule requires that the protons on the irons be able to approach each other and to form a bond.⁵ It is not necessary that the protonation take place on that part of the iron atoms that are best suited for close approach of the protons if there is a low-energy barrier for migration of the proton on the iron or for suitable bending modes of the protonated molecule.

Besides protonation of the iron atom, bridging the cyclopentadienyl rings of ferrocene with a trimethylene group forces the bridged rings to be tilted, in the bridging case by about 10° . Theory^{17,18} suggests that the projected orbitals that accommodate the protonation become accessible because of the tilting. Consequently, pretilting of the rings with bridges is expected to have some effect on the rates and/or the equilibrium constants of the protonation reactions. These effects have not been determined. A priori, in the absence of competing effects, it may be expected that both the rate of protonation and the equilibrium constant would increase. What can be assumed with some degree of certainty, however, is that the orientation of the protons on the iron is fixed by the direction of the tilting imparted by the short trimethylene bridge. Such control of the direction of protonation has been reported.¹⁹

If the proposed mechanism for the formation of dihydrogen from [1.1]ferrocenophanes is correct, then it should be possible to design ferrocenophane molecules that would exhibit either higher or lower overall rates. It was for this reason that the bridged ferrocenophanes II and III were prepared and their crystal structures determined.¹² Figure 5 gives views of the directions of the ring-tilt openings for the structures of I, II, and III. (The structure shown for I is an adaptation of that determined²⁰ for the

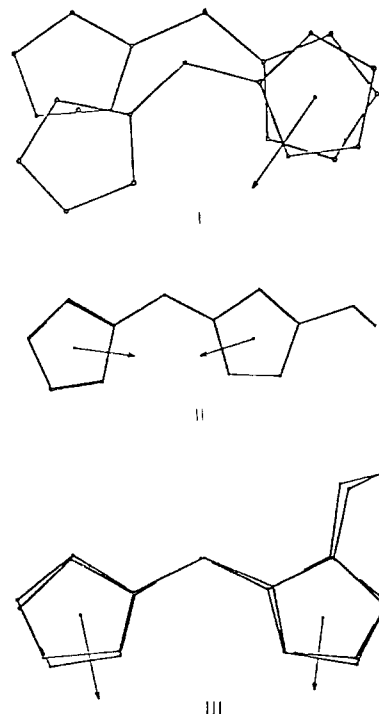


Figure 5. ORTEP views of compounds used in study showing directions of tilt openings. The ORTEP diagram of I is taken from that¹⁶ of the 11,12-dimethyl derivative with the methyls deleted. The ORTEP's of II and III are from the data in ref 8. Because of the relative twisting of the two ferrocene units of I, only one direction vector is shown. The other is not easily pictured. However, there is a crystallographic center of symmetry at the midpoint between the iron atoms, and the second vector can be inferred from that.

11,12-dimethyl derivative with the methyl groups deleted. Since the methyl groups are exo, it is not expected that there would be gross differences between the dimethyl derivatives and I.) Without any further considerations of other possible interactions, from these ring-tilt directions alone, the rates of dihydrogen formation should be faster for II and slowest for III. This is what was observed.

Some other considerations are as follows: The bridge, it would seem, imparts rigidity (direction of tilt opening) only to one of the ferrocene units. The other unit remains mobile as far as the proton on the iron atom is concerned. Dreiding models show that I is a very flexible molecule, while II and III are not, with III somewhat more rigid than II. The NMR spectra, however, by virtue of the averaging of the two conformationally different hydrogen atoms on the [1.1] methylene groups, show¹² that I and II are flexible. The NMR spectrum of III, on the other hand, has separate peaks for the two conformationally unique hydrogen atoms on the [1.1] methylenes, thus showing that the compound is rigid. From this, we can conclude that the high flexibility of I causes the rate of dihydrogen formation from it to be higher than would be expected from ring-tilt directions alone. The rate of dihydrogen formation from II is somewhat higher than expected from considerations of ring-tilt directions alone, and dihydrogen formation from III is essentially dependent on ring-tilt directions. This is borne out by the small difference in rates of dihydrogen formation from I and II as compared with the large difference between II and III.

In conclusion, these results give experimental support to the reaction scheme (eq 1-3) previously hypothesized.¹

(16) Hillman, M.; Kwick, A. *Organometallics* 1983, 2, 1780-1785.

(17) Ballhausen, C. J.; Dahl, J. P. *Acta Chem. Scand.* 1961, 1333-1336.

(18) Lauher, J.; Hoffman, R. *J. Am. Chem. Soc.* 1976, 98, 1729-1742.

(19) Bitterwolf, T. E.; Ling, A. C. *J. Organomet. Chem.* 1981, 215, 77-86.

(20) McKechnie, M.; Maier, C. A.; Bersted, B.; Paul, I. C. *J. Chem. Soc., Perkin Trans. 2* 1973, 138-143.

The orientation of the ring-tilt openings and/or the flexibility of the molecules appear to affect the rate of dihydrogen evolution. Since both geometrical effects have some control over the ability of the protons on the irons to approach each other, protonation of the iron atoms is apparently an essential part of the mechanism. It can be inferred from the electrochemical behavior of the system that the first protonation is fast. Only at the highest acidities is it possible to affirm that the elimination of

dihydrogen is the rate-determining step. At lower acidities, the second protonation may be comparably slow.

Acknowledgment. We are indebted to Drs. R. C. Kerber and J. Smalley for valuable discussions. This work was supported by the Division of Chemical Sciences, U.S. Department of Energy, Washington, D.C., under Contract No. DE-AC02-76CH00016.

Registry No. I, 1294-39-9; II, 90991-28-9; III, 90991-27-8.

New Organometallic Hydrido Nitrosyl Complexes of Tungsten^{1,2}

Peter Legzdins,* Jeffrey T. Martin, and Jimmie C. Oxley³

Department of Chemistry, The University of British Columbia, Vancouver, British Columbia, Canada V6T 1Y6

Received November 26, 1984

Treatment of dark purple $[\text{CpW}(\text{NO})\text{I}_2]_2$ ($\text{Cp} = \eta^5\text{-C}_5\text{H}_5$) with 1 or 2 equiv of $\text{Na}[\text{H}_2\text{Al}(\text{OCH}_2\text{CH}_2\text{OCH}_3)_2]$ in $\text{CH}_2\text{Cl}_2\text{-C}_6\text{H}_6$ affords green $[\text{CpW}(\text{NO})\text{IH}]_2$ or orange $[\text{CpW}(\text{NO})\text{H}_2]_2$, respectively, both products being isolable as analytically pure solids. Addition of PR_3 ($\text{R} = \text{Me, Ph, OMe or OPh}$) to any of the bimetallic nitrosyl complexes results in formation of the corresponding monometallic derivatives. Hence, $[\text{CpW}(\text{NO})\text{I}_2]_2$ is converted into brown $\text{CpW}(\text{NO})\text{I}_2(\text{PR}_3)$, $[\text{CpW}(\text{NO})\text{IH}]_2$ transforms into orange $\text{CpW}(\text{NO})\text{IH}(\text{PR}_3)$, and $[\text{CpW}(\text{NO})\text{H}_2]_2$ ultimately yields orange $\text{CpW}(\text{NO})\text{H}_2(\text{PR}_3)$. The latter compounds are formed via the intermediate complexes $[\text{CpW}(\text{NO})\text{H}(\text{PR}_3)]_2$, which can be isolated from C_6H_6 as purple microcrystals when $\text{R} = \text{OPh}$. The monomeric diiodo nitrosyl complexes may also be converted to their hydrido nitrosyl analogues by reaction with $\text{Na}[\text{H}_2\text{Al}(\text{OCH}_2\text{CH}_2\text{OCH}_3)_2]$. All new compounds synthesized have been characterized by conventional spectroscopic techniques, particularly ^1H NMR spectroscopy. The physical properties of the dimeric hydride complexes indicate that they all contain bridging hydride ligands and that they are best formulated as $[\text{CpW}(\text{NO})]_2(\mu\text{-I})_2(\mu\text{-H})_2$, $[\text{CpW}(\text{NO})\text{H}]_2(\mu\text{-H})_2$, and $[\text{CpW}(\text{NO})(\text{PR}_3)]_2(\mu\text{-H})_2$. Plausible molecular structures for these compounds and their monomeric derivatives are proposed.

Introduction

Current interest in the synthesis, characterization, and properties of organotransition-metal hydride complexes continues unabated, primarily because many important stoichiometric and catalytic chemical conversions have been demonstrated to involve metal-hydrogen linkages at key stages.⁴ In this regard, however, relatively little is known presently about how the physical and chemical properties of such linkages are affected by the presence of NO ligands in the metal's coordination sphere. This state of affairs simply reflects the paucity of well-defined organometallic hydrido nitrosyl complexes. The first report of such a species appeared in 1972 when Graham and coworkers communicated the existence of $\text{CpRe}(\text{CO})(\text{NO})\text{H}$ ($\text{Cp} = \eta^5\text{-C}_5\text{H}_5$).⁵ Since that time, only this compound,⁶ its PPh_3 derivative,⁷ $\text{CpW}(\text{NO})_2\text{H}$,⁸ $\text{HFe}(\text{CO})_2$ -

$(\text{NO})(\text{PPh})_3$,⁹ and $\text{HFe}(\text{CO})(\text{NO})(\text{PPh})_2$ ⁹ have been studied in any detail. Consequently, we have recently been endeavoring to develop synthetic routes to other members of this class of compounds.

As part of a previous study,¹⁰ we succeeded in synthesizing $\text{CpW}(\text{NO})\text{IH}[\text{P}(\text{OPh})_3]$ and $[\text{CpW}(\text{NO})\text{IH}]_2$, but in only 9% yield and of poor quality, respectively. We have now improved upon and extended this earlier work, and in this paper we wish to report superior preparations and characterizations of these two compounds as well as several other related hydrido nitrosyl complexes of tungsten.

Experimental Section

All manipulations were performed so as to maintain all chemicals under an atmosphere of prepurified dinitrogen either on the bench using conventional techniques for the manipulation of air-sensitive compounds¹¹ or in a Vacuum Atmospheres Corp. Dri-Lab Model HE-43-2 drybox. All chemicals used were of reagent grade or comparable purity. All reagents were either purchased from commercial suppliers or prepared according to published procedures, and their purity was ascertained by elemental analyses, melting point determinations, and/or other suitable methods. Melting points were taken in capillaries by using

(1) Organometallic Nitrosyl Chemistry. 25. For part 24 see: Hunter, A. D.; Legzdins, P.; Nurse, C. R.; Einstein, F. W. B.; Willis, A. C. *J. Am. Chem. Soc.* 1985, 107, 1791.

(2) Presented in part at the Can-Am Chemical Congress, June 1984, Montreal, Quebec.

(3) Present address: Department of Chemistry, New Mexico Institute of Mining and Technology, Socorro, NM 87801.

(4) Collman, J. P.; Hegedus, L. S. "Principles and Applications of Organotransition Metal Chemistry"; University Science Books: Mill Valley, CA, 1980.

(5) Stewart, R. P.; Okamoto, N.; Graham, W. A. G. *J. Organomet. Chem.* 1972, 42, C32.

(6) Sweet, J. R.; Graham, W. A. G. *Organometallics* 1982, 1, 982.

(7) Tam, W.; Lin, G.-Y.; Wong, W.-K.; Kiel, W. A.; Wong, V. K.; Gladysz, J. A. *J. Am. Chem. Soc.* 1982, 104, 141.

(8) Legzdins, P.; Martin, D. T. *Inorg. Chem.* 1979, 18, 1250.

(9) Rouston, J.-L. A.; Forgues, A.; Merour, J.-Y.; Yenayak, N. D.; Morrow, B. A. *Can. J. Chem.* 1983, 61, 1339.

(10) Hames, B. W.; Legzdins, P.; Oxley, J. C. *Inorg. Chem.* 1980, 19, 1565.

(11) Shriver, D. F. "The Manipulation of Air-Sensitive Compounds"; McGraw-Hill: New York, 1969.